Polymer Films Possessing Nanoreinforcements via Organically Modified Layered Silicate

Fawn M. Uhl,[†] Siva Prashanth Davuluri,[‡] Shing-Chung Wong,[‡] and Dean C. Webster*[,§]

Center for Nanoscale Science and Engineering, Department of Mechanical Engineering and Applied Mechanics, and Department of Polymers and Coatings, North Dakota State University, P.O. Box 5376, Fargo, North Dakota 58105-5376

Received November 7, 2003. Revised Manuscript Received January 21, 2004

UV-curable polymer films were prepared containing a commercially available, organically modified montmorillonite (MMT). It is believed that nanoclay-containing UV-curable polymers can find wide ranging applications in future microelectronic materials. Polymer films containing the commercially available MMT clay (Nanomer) exhibited enhancements in properties. The polymer films were studied with various microanalytical techniques including XRD, TEM, and SEM to determine their micromorphology. Physical properties and curing kinetics were examined using FTIR and thermal analysis. It was found that the incorporation of clay reduced cure time. Tensile modulus, strength, and glass transition temperature all increased with clay content. Dimensional stability improved with addition of clay. Adhesion between the UV-curable film and polysulfone substrate also dramatically improved. The presence of commercially modified MMT clay, however, rendered the polymers more susceptible to thermal degradation.

Introduction

Clay nanocomposites have typically been prepared by an in situ polymerization method or by a melt compounding method. It has been shown that polar polymers and monomers can intercalate directly into sodium montmorillonite. Some examples include poly(ethylene oxide) and methyl methacrylate monomer.[1] Blumstein showed that poly(methyl methacrylate) (PMMA) and sodium montmorillonite formed clay−polymer nanocomposites by in situ free radical polymerization.[2−4] He observed an increase in the *d*-spacing of the clay by 0.76 nm, indicating the formation of intercalated nanocomposites.[1−5] Improvement in thermal stability was also noted. Unlike polar polymers or monomers, nonpolar compounds are not readily miscible with sodium clay. Therefore, the clay is modified using an ion-exchange process in which the sodium ion is replaced with an organoammonium or phosphonium salt. This procedure makes the clay more organophilic and more miscible with nonpolar monomers and polymers. The clay nanocomposites obtained thus far have been shown to exhibit enhanced properties, such as improved mechanical, thermal, barrier, solvent resistance.[6−10]

Little work has been done on UV-curable polymer−clay nanocomposites. Zahouily et al. first demonstrated that UV-curable polymer−clay nanocomposites could be prepared.[11,12] Decker et al. showed by X-ray diffraction that clay nanocomposites can be prepared with UV-curable formulations.[13] Several advantages are associated with UV curing, such as rapid cure, solvent-free systems, application versatility, low energy requirements, and low-temperature operation.[14,15] For many microelectronic applications, it is desirable to formulate thin polymer systems with high glass transition temperatures, good barrier properties, dimensional stability, flexibility, and good mechanical properties.

The focus of this paper is on the preparation and characterization of UV-curable films possessing nanoreinforcements. Structure−property relationships are elucidated using a number of analytical techniques.

Experimental Section

Materials. Nanomer I.31PS onium ion modified montmorillonite was supplied by Nanocor Inc. CN929, a trifunc-

* Corresponding author. Phone: (701) 231-8709. Fax: (701) 231-8439. E-mail: Dean.Webster@ndsu.nodak.edu.
[†] Center for Nanoscale Science and Engineering.
[‡] Department of Mechanical Engineering and Applied Mechanics.
[§] Department of Polymers and Coatings.

(1) Gilman, J. W., Jr.; Harris, R.; Hunter, D., *44th Intl. SAMPE Symposium/Exhibition, Book 2;* 1999; pp 1408−1423.
(2) Blumstein, A. *J. Polym. Sci.: Part A* **1965**, *3*, 2653−2664.
(3) Blumstein, A. *J. Polym. Sci.: Part A* **1965**, *3*, 2665−2672.
(4) Blumstein, A. *J. Polym. Sci.: Part A-2* **1966**, *4*, 465−474.
(5) Gilman, J. W. *Appl. Clay Sci.* **1999**, *15*, 31−49.
(6) Alexandre, M.; Dubois, P. *Mater. Sci. Eng.* **2000**, *R28*, 1−63.
(7) Ogawa, M.; Kuroda, K. *Bull. Chem. Soc. Jpn.* **1997**, *70*, 2593−2618.
(8) Wang, W. J.; Chin, W.-K. *J. Polym. Sci. Part B: Polym. Phys.* **2002**, *40*, 1690−1703.
(9) Tortora, M.; Gorrasi, G.; Vittoria, V.; Galli, G.; Ritrovati, S.; Chiellini, E. *Polym.* **2002**, *43*, 6147−6157.
(10) Wu, J.; Lerner, M. M. *Chem. Mater.* **1993**, *5*, 835−838.
(11) Zahouily, K.; Benfarhi, S.; Bendaikha, T.; Baron, J.; Decker, C. *Proc. RadTech Europe* **2001**, 583.
(12) Zahouily, K.; Decker, C.; Benfarhi, S.; Baron, J. *Proc. RadTech North Am.* **2002**, 309−320.
(13) Decker, C.; Zahouily, K.; Keller, L.; Benfarhi, S.; Bendaikha, T.; Baron, J. *J. Mater. Sci.* **2002**, *37*, 4831−4838.
(14) Jackson, P. *Paint Resin Times* **2002**, *1*, 26−27.
(15) Fouassier, J. P., *Photoinitiation, Photopolymerization, and Photocuring Fundamentals and Applications*; Hanser Publishers: New York, 1995; p 246.

10.1021/cm035137d CCC: $27.50
Published on Web 02/27/2004

tional urethane acrylate oligomer, and SR454, an ethoxylated (3) trimethylolpropane triacrylate, were obtained from Sartomer. The photoinitiator, Darocur 1173, 2-hydroxy-2-methyl-1-phenylpropane-1-one, was obtained from Ciba Specialty Chemicals.

Characterization UV curing of samples was performed using a Dymax light source with a 200 EC silver lamp (UV-A, 365 nm). The intensity was 35 mW/cm^2 using a NIST Traceable Radiometer, International Light model IL1400A. It should be noted that curing of panels was performed in air. Samples were drawn down onto an aluminum panel using a #1 Gardco casting bar with a gap of 4 mil. X-ray powder diffraction (XRD) data were collected using a Phillips PW3040 X'pert-MPD multipurpose diffractometer in Bragg−Brentano geometry (Cu Kα radiation). Qualitative variable-slit data were collected over 2θ angles of 2°−40°, using a step size of 0.02 and a run time of 1 s/step. TEM samples were cut using a diamond knife and RMC MTXL ultramicrotome. The ultrathin sections were then placed on 400 mesh copper grids and photographed using a JEOL 100cx-II transmission electron microscope operating at 80 kV. Fourier transform infrared (FTIR) was done using a Nicolet Magna-IR 850 spectrometer series II with detector type DTGS KBr. Scans were done in transmission mode from 4000 to 400 cm^{-1}. Photoinfrared was performed using the Nicolet spectrometer and a UV optic fiber mounted in a sample chamber. The light source was a 100 W DC mercury vapor short-arc lamp. This setup monitors the conversion as the reaction proceeds and is known as real-time infrared spectrometry (RTIR). Samples were applied to a KBr disk by spin coating. Scans were taken over a 60 s period at 1 scan/s and the UV source was adjusted to be approximately 3.6 mW/cm^2 and performed in air. Differential scanning calorimetry (DSC) was performed on a TA Instruments Q1000 series calorimeter. Samples were subjected to a heat−cool−heat cycle from −20 to 200 °C at a ramp rate of 10 °C/min. T_g values were determined as the midpoint of the inflection from the second heat cycle. Photo-DSC was performed utilizing the Q1000 DSC modified with the photocalorimic accessory (PCA) and its intensity was approximately 40 mW/cm^2 in a nitrogen atmosphere. Sample sizes ranged from 4 to 6 mg. The reproducibility of photo-DSC has been found to be ±3%. Dynamic mechanical thermal analysis (DMTA) was performed using a Rheometric Scientific 3E apparatus in the rectangular tension/compression geometry. T_g is obtained from the maximum peak in the tan δ curves, and cross-link densities are calculated from the E' value in the linear portion at least 50 °C greater than the T_g. Cross-link density can be calculated from the following equation[16]

$$E = 3\nu_e RT \qquad (1)$$

where ν_e is the cross-link density.

Sample sizes for testing were 10 × 5 × (0.05 to 0.09) mm^3. The analysis was carried out from −50 to 250 °C at a frequency of 10 rad/s and a ramp rate of 5 °C/min. Thermogravimetric analysis (TGA) was performed using a Perkin-Elmer-7 under nitrogen purging from ambient temperature to 800 °C at a ramp rate of 20 °C/min. Tensile properties were measured using an Instron 5542, and five specimens were taken for each sample to obtain an average value following ASTM 2370. Test specimens for the tensile tests were free films with a length of 100 mm, and grips were set to a distance of 40 mm. The width of the samples was 5 mm and thickness 0.05−0.09 mm. A crosshead speed of 20.0 mm/min was applied. Coefficient of thermal expansion was obtained using a TA 2940 thermomechanical analyzer (TMA). The force applied was 0.003 N and it was heated at a rate of 5 °C/min from room temperature to 100 °C. Hardness tests were performed utilizing a BYK Gardener pendulum hardness tester in the König mode in seconds. Samples for hardness testing were cured on an aluminum panel. Adhesion testing was performed using a portable adhesion tester following ASTM procedure D4541. In this case, a dolly is attached to a surface of a coating with an epoxy adhesive, Araldite 2011. Tension is applied perpendicular to the surface and the force applied to the loading fixture is increased until the coating is removed from the substrate. The force required to remove the coating is recorded in lb/in^2.

Formula	
Gamma-aminopropyltriethoxysilane	0.5 – 5 wt %
Octadecylamine	35 – 15 wt %
MMT clay	65 – 85 wt %

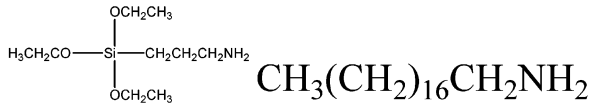

Figure 1. Structure and composition of modified MMT clay.

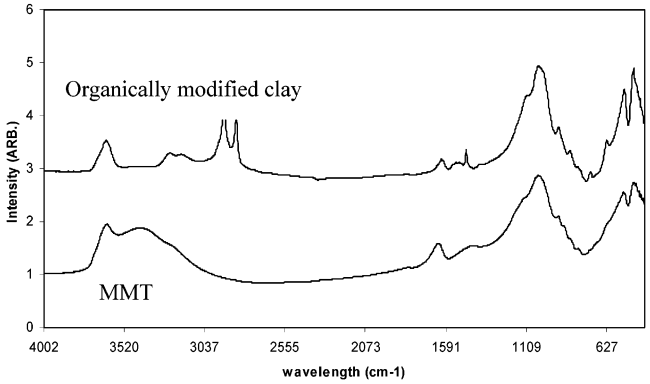

Figure 2. FT-IR spectrum of unmodified montmorillonite (MMT, bottom) and modified MMT clay (top).

Preparation of Nanocomposite Polymer Films. Polymer film formulations utilized in this study were a 50:50 mixture of CN929:SR454. CN929 is a trifunctional aliphatic polyester urethane acrylate oligomer. SR454 is an ethoxylated timethylolpropane triacrylate. The clay loadings in these systems were 1, 3, and 5 wt %. The mixture was stirred for 24 h followed by sonication for 8 h. Then the initiator Darocur 1173(4 wt %) was added and mixture stirred overnight. Films were cast onto glass, aluminum, and polysulfone panels using a #1 Gardco casting bar with a gap of 4 mil.

Results and Discussion

The presence of nanoclays has been shown to enhance polymer properties.[6−10] Properties desired for polymer substrates and laminating layers in electronic applications are good barrier, dimensional stability, flexibility, good mechanical properties, and high T_g. UV curing of polymers is an attractive route for microelectronic packaging materials. In a series of papers,[17] we are seeking to address the important aspects of developing polymer nanocomposite films for UV-curable polymer systems. The research can impact on future development of microelectronic polymeric components using clay-type nanocomposites. The structure−property relationships of such nanocomposites are emphasized herein.

Structure of Commercially Modified Montmorillonite Clay. Organic modification is typically employed in clay−polymer nanocomposites. The clay used in this study was Nanomer I.31 PS, a commercially

(16) Wicks, Z. W., Jr.; Jones, F. N.; Pappas, S. P. *Organic Coatings*; John Wiley & Sons: New York, 1999; p 71.

(17) Uhl, F. M.; Hinderliter, B. R.; Davuluri, S. P.; Croll, S. G.; Wong, S.-C.; Webster, D. C. *Polym. Prepr.* **2003**, *44(2)*, 247−248.

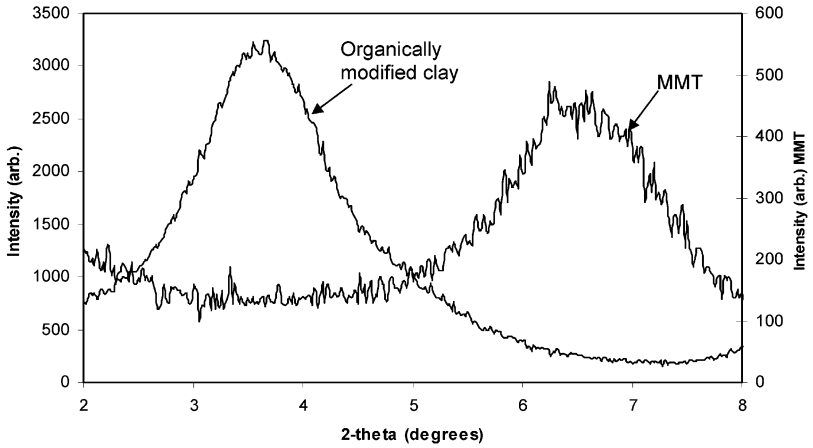

Figure 3. XRD patterns of MMT and modified MMT clay.

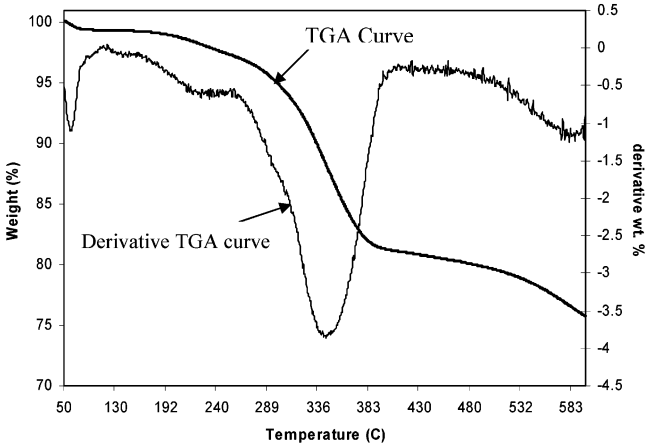

Figure 4. TGA curve of modified MMT clay.

available montmorillonite clay, from Nanocor Inc. The montmorillonite clay contains γ-(aminopropyl)triethoxysilane and octadecylamine as the organic modifiers (Figure 1). FT-IR data demonstrate that the organic modifiers are present in the montmorillonite clay. Figure 2 shows FT-IR spectra of unmodified montmorillonite (MMT) and of the commercially modified MMT clay, where new peaks attributable to the organic modifiers are observed at 3240 and 3174 cm^{-1}, due to the NH stretching, and at 2912 and 2839 cm^{-1}, due to the CH stretching.

X-ray Diffraction (XRD). X-ray diffraction shows that there is an increase in the *d*-spacing of the commercially modified MMT clay compared to the unmodified MMT, as shown in Figure 3. The *d*-spacing of the montmorillonite is 1.34 nm and upon organic modification the *d*-spacing for commercially modified MMT clay increases to 2.41 nm, which is an increase of 80%. The increase in *d*-spacing (1.07 nm) is attributable to the organic modifiers being incorporated between the clay layers and pushing the clay layers further apart, resulting in an intercalated structure. In this case an intercalated structure is formed, showing that organomodification alone is not sufficient to exfoliate the clay.

Thermogravimetric Analysis (TGA). The thermal stability of the commercially modified MMT clay is shown in Figure 4. There is an initial loss of approximately 1% below 100 °C, possibly due to the loss of water. At 600 °C, the amount of char remaining is 76%, indicating a mass loss of 24%. The amount of organic modifier present is reported to be between 20 and 35%. In the case of unmodified montmorillonite, we have observed a mass loss of approximately 10% below 150 °C, which is attributed to the loss of water.[18] There are no further losses above 150 °C for the unmodified montmorillonite.[18] Mass loss for the clay is within this range and can be attributed to the loss of organic modifier present in the montmorillonite clay.

Table 1. XRD Information for Clays and Polymer Film Formulations

sample	*d*-spacing (nm)	% increase in *d*-spacing relative to MMT	% increase in *d*-spacing relative to modified MMT
MMT	1.34	NA	NA[b]
cm-MMT[a]	2.41	44	NA
1 wt % cm-MMT			
3 wt % cm-MMT	3.25	143	35
5 wt % cm-MMT	3.34	149	39

[a] cm-MMT = commercially modified MMT. [b] Not applicable.

Structure of Nanoreinforced Films. *X-ray Diffraction (XRD).* Incorporation of the organic modifiers into the montmorillonite increases the *d*-spacing by 80%. Organically modified clay should be more readily miscible with monomers and polymers than unmodified clay. Table 1 shows the *d*-spacing values observed in the commercially modified MMT clay-containing polymer film. From this it is observed that at the 1 wt % loading a highly intercalated structure forms, as there is no peak observed in this case. The absence of an XRD peak does not necessarily mean exfoliation, as the observed absence of scattering could be due to geometry effects or lack of sensitivity at the low level of clay incorporation. At 3 and 5 wt % loading, peaks are observed at 3.25 and 3.34 nm, respectively, indicating that an intercalated structure is formed.

Transmission Electron Microscopy (TEM). To conclusively determine the morphology of the clay in the composite, direct observation using transmission electron microscopy is required. Figure 5 shows the TEM photomicrographs of 1 and 3 wt % Nanomer-reinforced urethane acrylate composites. In these cases the clay appears to be intercalated with some folded features, possibly resulting from the microtoming process. The degree of intercalation is quite high, almost to the extent

(18) Uhl, F. M.; Davuluri, S. P.; Wong, S.-C.; Webster, D. C. Manuscript in preparation.

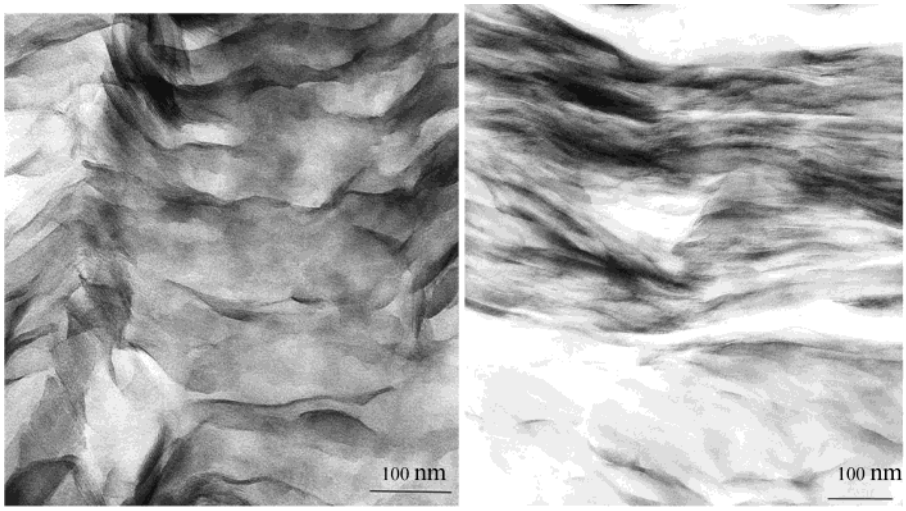

Figure 5. TEM of polymer film containing (a) 1% and (b) 3% modified MMT clay.

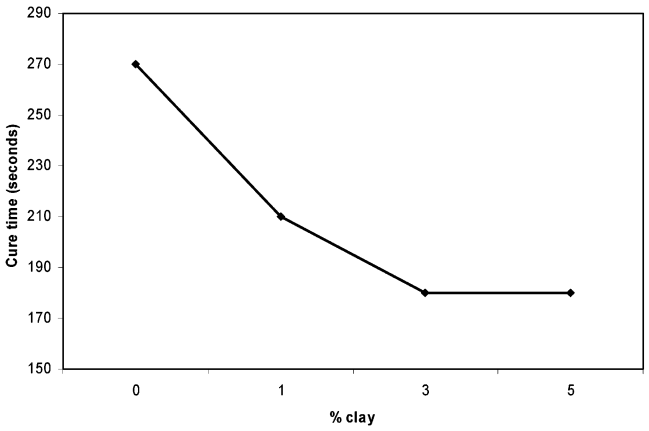

Figure 6. Cure times of unmodified and modified MMT containing polymer films.

of exfoliation. Dispersion appears to be better in the 1 wt % commercially modified MMT case than in the 3 wt % case. Both XRD and TEM confirm that polymer is indeed intercalated between the nanoclay sublayers.

Polymer Film Properties. Researchers have reported that an improvement in polymer properties is observed when clay is used as a form of nanoreinforcement.[6−10,19−24] Therefore, it is of interest to investigate the properties typically enhanced by the presence of nanoclay as well as the effect of nanocomposite formation on properties specifically associated with UV-curable polymer films.

Cure Time. The cure time of the unmodified polymer film is 270 s. Addition of the commercially modified MMT clay appears to decrease the cure time, as shown in Figure 6. Curing is the cross-linking of a polymer to produce a three-dimensional network that is tack free. We have previously shown that cure time is related to the type of organomodification of the clay.[25] A more significant decrease in cure time was exhibited when a single long chain (C_{16}) was attached to the ammonium ion.[18] As the amount of clay is increased, the cure time is decreased with a leveling effect at 3 wt % loading. This reduction in cure time as clay loading increases suggests that the presence of clay enhances the curing reaction. Since a number of factors could be impacting this macroscopic property, a more detailed investigation into the kinetics of the curing process is warranted.

Curing Kinetics. In UV-curable formulations the functional group conversion can be monitored by real-time infrared spectroscopy (RTIR) and photodifferential scanning calorimetry (photo-DSC). These two techniques monitor the cross-linking reactions taking place. In the case of RTIR, the loss due to a particular functional group in the infrared spectrum can be followed and related to the conversion. Photo-DSC monitors the UV curing reaction occurring by monitoring the heat flow between a reference and sample pan. Conversion is obtained by examining the area under the curve.

In RTIR, acrylate systems are typically monitored by the disappearance of the =C−H out-of-plane bend at 810 cm^{-1}. Figure 7 shows a typical plot obtained for the unmodified polymer film and polymer films containing 1, 3, and 5 wt % commercially modified MMT clay. From the initial portion of the RTIR plot (10 s or less), the rate of polymerization can be calculated. The degree of conversion and the estimated rate of polymerization (R_p) can be calculated on the basis of the following equations:[26−28]

$$\text{degree of conversion} = (((A_{810})_0 - (A_{810})_t)/(A_{810})_0) \times 100 \quad (2)$$

$$R_p = [M_0][((A_{810})_{t_1} - (A_{810})_{t_2})/(t_2 - t_1)] \quad (3)$$

(19) Chin, I. J.; Thurn-Albrecht, T.; Kim, H. C.; Russell, T. P.; Wang, J. *Polymer* **2001**, *42*, 5947−5952.
(20) Wang, Z.; Pinnavaia, T. J. *Chem. Mater.* **1998**, *10*, 3769−3771.
(21) Feng, W.; Ait-Kadi, A.; Riedl, B. *Polym. Eng. Sci.* **2002**, *42*, 1827−1835.
(22) Lan, T.; Kaviratna, D.; Pinnavaia, T. J. *Chem. Mater.* **1994**, *6*, 573−575.
(23) Mark, J. E.; Erman, B. *Rubberlike Elasticity. A Molecular Primer*; John Wiley & Sons: New York, 1988; p 145.
(24) Elias, H.-G., *Macromolecules 2nd Edition: Synthesis, Materials, and Technology*, Plenum Press: New York, 1984; p 1124−1128.
(25) Uhl, F. M.; Davuluri, S. P.; Wong, S.-C.; Webster, D. C. Manuscript in preparation.
(26) Stowe, F. S.; Lieberman, R. A. *J. Radiat. Curing* **1987**, *14*, 10−19.
(27) Decker, C.; Moussa, K. *Makromol. Chem.* **1988**, *189*, 2381−2394.

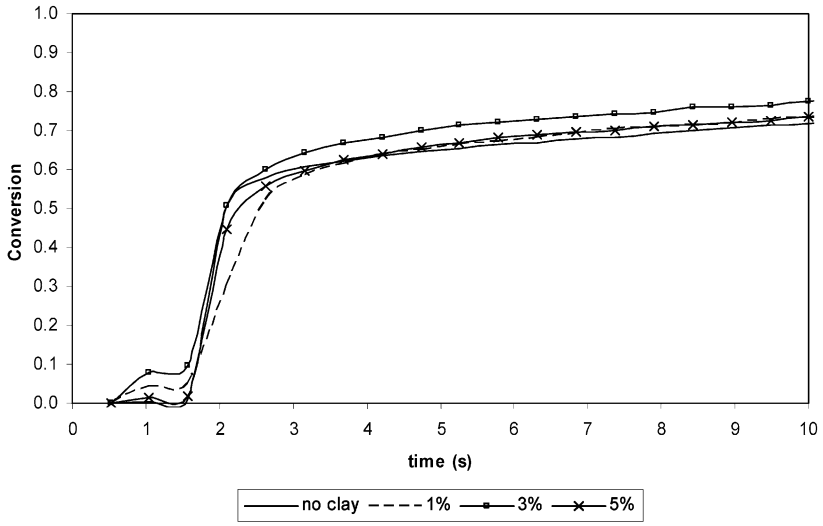

Figure 7. RTIR plot obtained for unmodified polymer film and polymer films containing modified MMT clay (exposure time 60 s, UV intensity 3.6 mW/cm^2).

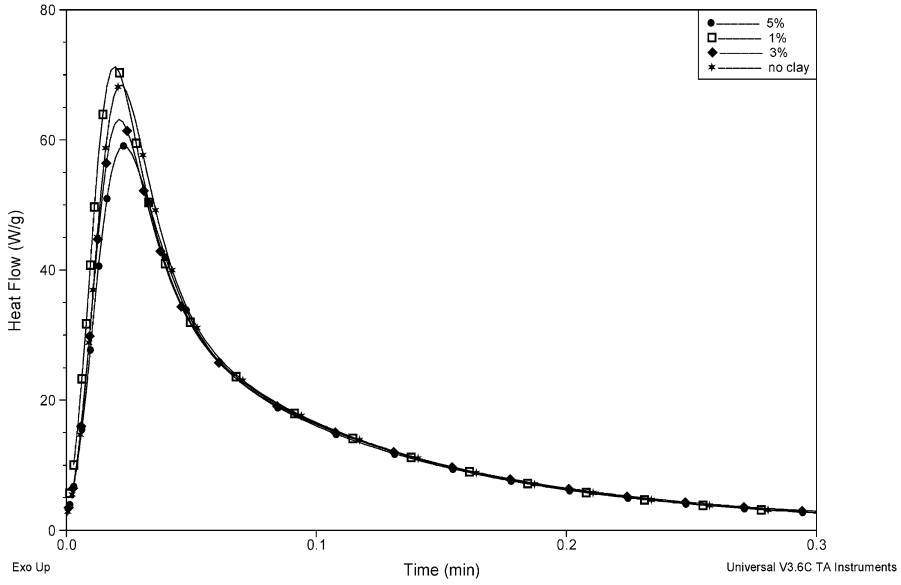

Figure 8. Photo-DSC plot of polymer films.

Table 2. Conversion and Rate of Polymerization for Polymer Films by RTIR, Averaged over 2 s[a]

	% conversion		
sample	at 10 s	at 60 s	R_p (mol/L s)
no clay	72	89	0.30
1% clay	73	90	0.39
3% clay	77	93	0.43
5% clay	74	89	0.32

[a] UV intensity 3.6 mW/cm^2. Clay represents the commercially modified MMT.

where $(A_{810})_0$ is the absorbance before UV exposure, $(A_{810})_t$ is the absorbance after UV exposure, $[M_0]$ is the original concentration of acrylate double bonds, and R_p is the rate of polymerization.

Table 2 shows the conversion obtained at 60 s and the rate of polymerization, R_p, which is the average R_p up to 2 s of exposure, as a function of the clay content. It should be noted that as clay is added into the formulation, a very slight increase in conversion is observed, similar to that observed by Zahouily et al.[12] and Decker et al.[13]

From the data in Table 2 it is observed that a slight increase in the estimated rate of polymerization occurs upon incorporation of clay. Photopolymerization of liquid crystalline media has been shown to result in a high yield, attributed to the reduction in termination rate where the translational and rotational movements are restricted,[29] indicating that the reduced mobility leads to reduced termination rate. In nanocomposite systems, the clay is capable of restricting the mobility of the polymer chains, resulting in a reduced rate of termination, leading to a higher rate of polymerization.

In photo-DSC, the heat flow and total heat evolved are measured. Total heat evolved can be related to the final degree of cure and is measured as the area under the curve. Figure 8 shows typical photo-DSC curves, where the maximum is denoted H_{max} and can be related

(28) Decker, C.; Moussa, K. *Makromol. Chem., Rapid Commun.* **1990**, *11*, 159−167.

(29) Hoyle, C. E.; Chawla, C. P.; Kang, D.; Griffin, A. C. *Macromolecules* **1993**, *26*, 758−763.

Table 3. H_{max} and Conversion (ΔH) for Polymer Films by Photo-DSC[a]

sample	H_{max} (W/J)	ΔH (J/g) [% conv]
no clay	68	246 [90]
1% clay	71	231 [85]
3% clay	63	232 [85]
5% clay	59	234 [86]

[a] There is a 3% error for measurements Clay represents the commercially modified MMT.

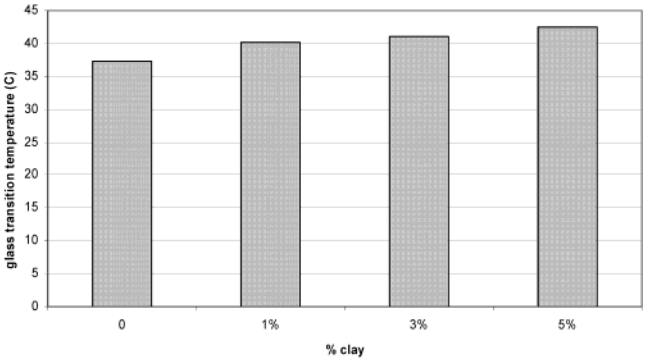

Figure 9. Glass transition temperatures by DSC.

to the rate of polymerization. Table 3 contains the H_{max} and area under the curve values obtained in photo-DSC. It is observed that at the 1 wt % loading of commercially modified MMT the rate is higher than that of the unmodified polymer film. As the amount of the commercially modified MMT is increased, the H_{max} value is lower than that of the unmodified polymer films, indicating a decrease in rate relative to the unmodified polymer film. When looking at the conversion (area under the curve), it is observed that all clay-containing polymer films have lower conversion than the unmodified polymer film. Conversion of the samples is in the following order: no clay > 5% clay > 3% clay > 1% clay. It appears that, at higher loadings of clay, conversion is higher, suggesting that commercially modified MMT clay is providing a significant interfacial area in the polymer, resulting in a higher rate of polymerization and heat evolved.

Thermal Properties. It has been shown for clay−polyimide nanocomposites that exfoliation occurs at low loadings and intercalation at high loadings.[30−32] A decrease in both the thermal expansion coefficient and gas permeability has been observed along with an increase in Young's modulus. Other investigators have also examined clay−epoxy nanocomposites and observed an increase in the glass transition temperature related to the amount of organoclay.[21,33,34]

Figure 9 shows the glass transition (T_g) temperatures obtained by DSC for the radiation-cured polymer films. The polymer films containing commercially modified MMT clay have a higher T_g than that of the virgin polymer film. The increase in T_g is attributed to the confinement of the polymer chains between the clay layers limiting segmental motion of the polymer chain.[3,7]

(30) Ranade, A.; D'Souza, N. A.; Gnade, B. *Polymer* **2002**, *43*, 3759−3766.
(31) Hsiao, S.-H.; Liou, G.-S.; Chang, L.-M. *J. Appl. Polym. Sci.* **2001**, *80*, 2067−2072.
(32) Agag, T.; Koga, T.; Takeichi, T. *Polymer* **2001**, *42*, 3399−3408.
(33) Wang, M. S.; Pinnavaia, T. J. *Chem. Mater.* **1994**, *6*, 468−474.
(34) Lan, T.; Kaviratna, D.; Pinnavaia, T. J. *Chem. Mater.* **1995**, *7*, 2144−2150.

Table 4. Glass Transition Temperatures and Cross-Link Density (XLD) by DMTA[a]

	run 1		run 2	
sample	T_g (°C)	XLD (mol/cm^3)	Tg (°C)	XLD (mol/cm^3)
no clay	73.9	6.0×10^{-3}	75.1	6.8×10^{-3}
1% clay	75.0	7.5×10^{-3}	75.1	7.4×10^{-3}
3% clay	75.1	8.3×10^{-3}	75.1	7.8×10^{-3}
5% clay	75.0	7.5×10^{-3}	73.9	8.3×10^{-3}

[a] Samples were run in duplicate and values for both runs are given. Clay represents the commercially modified MMT.

Table 5. DMTA Storage Modulus Data above and below the Glass Transition Temperatures[a]

	E' (GPa)	
sample	40 °C	175 °C
no clay	1.06	0.0697
1% clay	1.23	0.0799
3% clay	1.18	0.0874
5% clay	1.28	0.0844

[a] (Clay represents the commercially modified MMT)

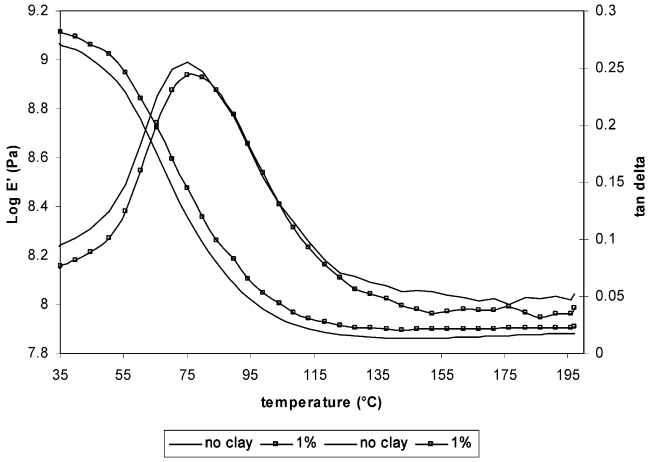

Figure 10. DMTA plot of unmodified coating and coating containing 1% modified MMT clay.

Dynamic mechanical analysis is a common technique to examine the viscoelastic behavior of polymer systems, including the glass transition behavior and also to obtain the cross-link density. Data for these films is shown in Table 4. T_gs obtained by DMTA are approximately the same for the clay-containing polymer films compared to the unmodified polymer film. It can be observed that as clay is incorporated into the formulation, an increase in the effective cross-link density (XLD) occurs. In general, the increase in XLD is related to the amount of clay present; as the amount of clay increases, the XLD increases. The results suggest that the presence of nanoclay can facilitate cross-linking reactions and thereby cross-link density is increased or that the clay is acting as a cross-link. It is well-known that physical aggregation of polymer chains onto the surface of a particulate results in a rise in the effective degree of cross-linking and this is likely what we are observing.[23]

Examination of the storage modulus, E', above and below the glass transition temperature can be carried out, and the results are shown in Table 5. Below the T_g (40 °C) E' is higher for the clay-containing polymer films than for the unmodified polymer film (Figure 10); this is an increase in E' of 10−20% at 40 °C. When looking

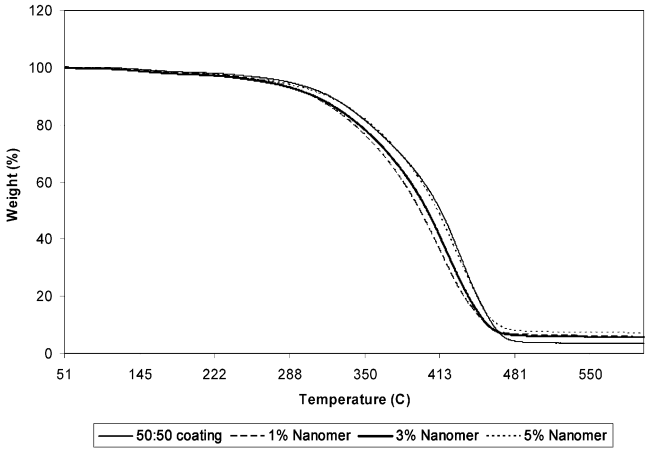

Figure 11. TGA curves for unmodified and clay-containing polymer films.

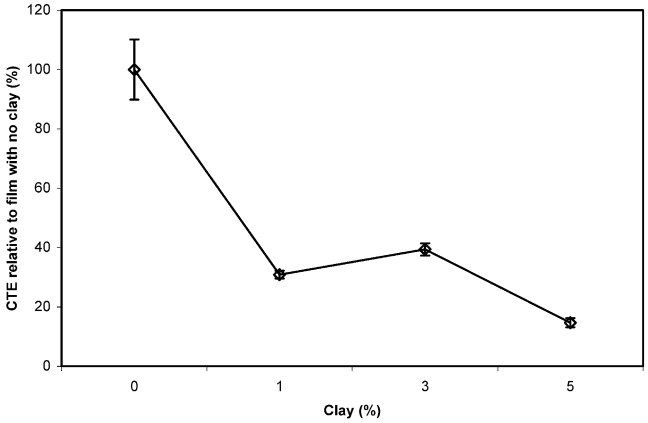

Figure 12. Coefficient of thermal expansion relative to unmodified film.

at E' above the T_g (175 °C), it is observed that at the various loadings of clay E' is again higher than that of the unmodified polymer film; in this case, an increase of 15−20% is observed. It should be noted that the tan δ curves for the unmodified polymer film is slightly broader than that of the clay-containing polymer films (Figure 10).

Degradation Behavior. Good thermal stability is required in processing and applications for microelectronic polymers and therefore is of importance in these materials. Figure 11 shows the TGA curves obtained. The clay-containing polymer films possess good thermal stability to approximately 320 °C. Formulations containing 1 and 3 wt % commercially modified MMT clay, however, have slightly lower thermal stability than that of the virgin polymer film, while the 5 wt % has the same thermal stability as the unmodified polymer film. All clay-containing polymer films exhibit a larger amount of char formation than the unmodified polymer film due to the presence of clay.

Coefficient of Thermal Expansion (CTE). The coefficient of thermal expansion (CTE) was obtained from thermomechanical analysis. In this particular case a decrease in CTE is observed upon addition of commercially modified MMT clay, as shown in Figure 12. A 60−85% decrease is observed for the commercially modified MMT containing polymer films relative to the unmodified polymer film. The results indicate that the incorporation of the commercially modified MMT clay can reduce CTE and provide good dimensional stability for the polymer films in this application.

Table 6. Mechanical Properties[a]

sample	elongation (mm)	yield strength (MPa)	Young's modulus (GPa)
no clay	2.5 ± 0.56	29.6 ± 1.7	0.990 ± 0.064
1% clay	3.5 ± 0.16	29.4 ± 0.88	1.09 ± 0.032
3% clay	2.3 ± 0.17	33.8 ± 1.4	1.28 ± 0.034
5% clay	2.2 ± 0.19	37.8 ± 2.1	1.49 ± 0.085

[a] Clay represents the commercially modified MMT.

Table 7. Hardness Data Compared to Other Data[a]

sample	König hardness (s)	T_g DSC (°C)	Young's Modulus (GPa)
no clay	89 ± 1.5	37.3	0.990 ± 0.064
1% clay	73 ± 1.2	40.2	1.09 ± 0.032
3% clay	76 ± 3.2	41.1	1.28 ± 0.034
5% clay	70 ± 6.1	42.4	1.49 ± 0.085

[a] Clay represents the commercially modified MMT.

Mechanical Properties. Typically, an improvement in mechanical properties is observed in polymer−clay nanocomposite systems. This is especially true in the case of the Young's modulus, because stiffness characterizes the initial deformation in the linear elastic regime. Table 6 displays the Young's modulus, tensile strength, and ductility values obtained from the samples studied. An increase in stiffness is observed as the amount of clay is increased. A 10% increase in modulus occurs at 1 wt % loading of commercially modified MMT and increases up to a 50% enhancement at the 5 wt % loading. This is in agreement with observations by DMTA, where an increase in E' is observed in the presence of clay. It can also be seen that as the amount of clay is increased, there is an increase in the tensile strength. Percent elongation of the polymer films decreases as the amount of commercially modified MMT is increased. Filler particles are known to reduce molecular mobility of polymer chains and lead to a less flexible material with a higher tensile strength and Young's modulus.[24] The reinforcement effect increases with increasing volume fraction of filler, and the more finely distributed the filler, the greater the effect.[24] Elongation is higher in the 1% case and approximately the same in the 3% and 5% cases compared to the unmodified coating.

Hardness. The hardness of the polymer films was determined using the König pendulum hardness test. In this test a pendulum swings back and forth and the time required to dampen the movement from a high (6°) to low (3°) angle is recorded. In this study the hardness of the polymer films containing clay are lower than that of the unmodified polymer film (Table 7). Sato has shown that the hardness of a polymer film can be related to other properties, such as the mechanical properties, of a polymer film.[35] Table 7 compares the hardness, T_g, and Young's modulus, while Table 5 list the E' values. From this it can be observed that for a low value of E' (from DMTA) a high hardness value is observed.[35] Sato observed that the data obtained from the "free torsional oscillation method" corresponded to that obtained by the pendulum hardness test; when a low shear modulus was observed, there was a higher

(35) Sato, K. *Prog. Org. Coat.* **1980**, *8*, 1−18.

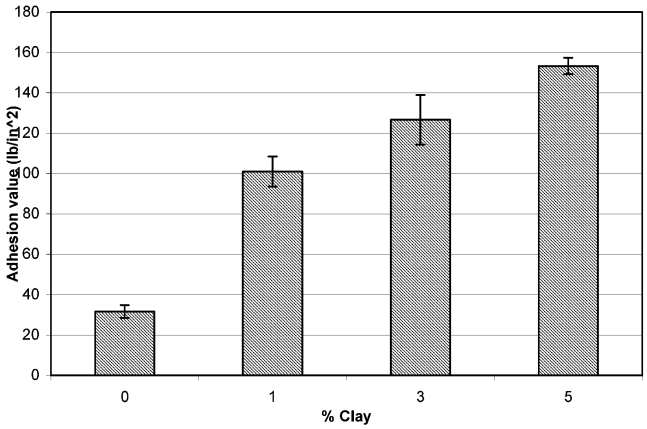

Figure 13. Pull-off adhesion values as a function of clay content.

hardness value observed. Our data correlates well with this observation; hardness values are highest for the unmodified film and lowest for the 5 wt % commercially modified MMT, and the E' values are lowest for the unmodified film and highest for the 5 wt % commercially modified MMT. The commercially modified MMT containing polymer films exhibit a decrease in hardness as the T_g is increased. From the data presented in Table 7, it is seen that as the Young's modulus is increased, there is a decrease in hardness.

Adhesion. Adhesion is the bonding between a polymeric coating and a substrate and it is the reversible separation of the two phases that is expressed by the work of adhesion.[36] In this study the adhesion of our polymer films (after curing) to a commercial polysulfone is measured. A significant increase in adhesion of the clay-containing polymer films is observed. This increase is related to the amount of clay present (Figure 13). This finding is interesting and warrants more detailed investigation in the future.

(36) Nelson, G. L. *Paint and Coating Test Manual*; ASTM: Philadelphia, 1995; p 513−525.

Conclusions

Structure and properties of UV-curable clay−urethane acrylate films were studied. Novel observations were made on UV-curable systems with commercially modified clays as the dispersed phase. TEM shows that intercalated structures were formed, but the clay platelets are highly intercalated nearing exfoliation. The formation of these nanoreinforced polymer films has led to enhanced properties. Tensile modulus, strength and to a small extent T_g increased as clay content increased. A decrease in cure time was observed upon incorporation of the clay. The coefficient of thermal expansion decreased with an increase in clay content. The result showed good dimensional stability as a function of temperature. Adhesion between UV-curable film and polysulfone substrate also showed dramatic improvement upon addition of clay particles.

Acknowledgment. The authors thank the Center for Nanoscale Science and Engineering (CNSE) and the Defense Microelectronics Activity (DMEA), contract number DMEA-90-02-C-0224, for support of this research. One of us (S.C.W.) acknowledges the support of NSF SGER Grant No. CMS 0335390 on nanocomposites administered by the Mechanics and Materials Program.

CM035137D